



RESEARCH ARTICLE

The effect of westerlies on East African rainfall and the associated role of tropical cyclones and the Madden–Julian Oscillation

Declan L. Finney¹  | John H. Marsham^{1,2} | Dean P. Walker¹ | Cathryn E. Birch¹ |
Beth J. Woodhams¹  | Lawrence S. Jackson¹ | Sam Hardy¹

¹School of Earth and Environment,
University of Leeds, Leeds, UK

²National Centre for Atmospheric
Science, Leeds, UK

Correspondence

*D. L. Finney, School of Earth and
Environment, University of Leeds, Leeds
LS2 9JT, UK.

Email: d.l.finney@leeds.ac.uk

Funding information

Department for International
Development, NE/M020126/1,
NE/M02038X/1, NE/MO17176/1; Natural
Environment Research Council,
NE/L002574/1, NE/M020126/1,
NE/M02038X/1, NE/MO17176/1,
NE/N008227/1; UK research and
innovation, NE/P021077/1

Abstract

Variability of rainfall in East Africa has major impacts on lives and livelihoods. From floods to droughts, this variability is important on short daily time-scales to longer decadal time-scales, as is apparent from the devastating effects of droughts in East Africa over recent decades. Past studies have highlighted the Congo airmass in enhancing East African rainfall. Our detailed analysis of the feature shows that days with a westerly moisture flow, bringing the Congo airmass, enhance rainfall by up to 100% above the daily mean, depending on the time of year. Conversely, there is a suppression of rainfall on days with a strong easterly flow. Days with a westerly moisture flux are in a minority in all seasons but we show that long rains with more westerly days are wetter, and that during the most-recent decade which has had more frequent droughts (associated with the “Eastern African climate paradox”), there has been few days with such westerlies. We also investigate the influence of the Madden–Julian Oscillation (MJO) and tropical cyclones, and their interaction with the westerly flow. We show that days of westerly moisture flux are more likely during phases 3 and 4 of the MJO and when there are one or more tropical cyclones present. In addition, tropical cyclones are more likely to form during these phases of the MJO, and more likely to be coincident with westerlies when forming to the east of Madagascar. Overall, our analysis brings together many different processes that have been discussed in the literature but not yet considered in complete combination. The results demonstrate the importance of the Congo airmass on daily to climate time-scales, and in doing so offers useful angles of investigation for future studies into prediction of East African rainfall.

KEYWORDS

Congo airmass, East Africa, long rains, Madden–Julian Oscillation, rainfall, tropical cyclones

This is an open access article under the terms of the Creative Commons Attribution License, which permits use, distribution and reproduction in any medium, provided the original work is properly cited.

© 2019 The Authors. *Quarterly Journal of the Royal Meteorological Society* published by John Wiley & Sons Ltd on behalf of the Royal Meteorological Society.

1 | INTRODUCTION

The severe societal impacts of droughts and floods in East Africa are well documented in the media and scientific literature (Kilavi *et al.*, 2018). Floods can lead to the spreading of water-borne diseases, as well as damage infrastructure and crops (ACAPS, 2018; Kilavi *et al.*, 2018; The Guardian, 2018). But in more recent decades, droughts have been prevalent during the long rains (March–May), and these recent dry decades have been extensively studied (Maidment *et al.*, 2015; Rowell *et al.*, 2015; Hoell *et al.*, 2017; Wainwright *et al.*, 2019). The apparent conflict between the recent dry period and climate projections of increased rain has been referred to as the “Eastern African Climate Paradox” (Rowell *et al.*, 2015; Wainwright *et al.*, 2019). Understanding the processes that control the large variability in East Africa long rains is essential to provide reliable warnings and forecasts to the population, as well as to be able to assess confidence in projections of climate change in the region.

The Rift Valley is a dominant feature of East Africa. At the heart of the Rift Valley is Lake Victoria, the largest tropical lake. There are large mountains to the east and to the west of the lake, and beyond these lie the Indian Ocean coastline and the Congo rainforest, respectively. The three main moisture sources for weather in East Africa are therefore the Indian Ocean, Lake Victoria, and the humid boundary layer of the Congo airmass. Broadly speaking a westerly flow of moisture across East Africa can be considered to import the Congo airmass, and an easterly flow to import the Indian Ocean airmass. The average flow has an easterly component in all seasons, with transitions between a northerly and southerly component twice a year as the tropical rainband crosses the Equator during the long (March–May) and short (October–December) rains (Yang *et al.*, 2015).

Westerly wind anomalies have been associated with enhanced rainfall over East Africa (specifically, the highland region) in studies of flooding events (Anyamba, 1983), seasonal variability (Camberlin and Wairoto, 1997), the Madden–Julian Oscillation (MJO; Pohl and Camberlin, 2006; Berhane and Zaitchik, 2014; Hogan *et al.*, 2015), and climate change (Giannini *et al.*, 2018). However, the idea of absolute westerly flow from the Congo has been described to some extent in only the studies of the MJO. The MJO is an eastward propagating atmospheric wave which suppresses and enhances tropical convection, with the location of convection/suppression depending on the phase of the wave. It has been shown that the majority of East Africa (in particular, the highlands) experience enhanced rainfall during phases 2–4 of the MJO (Hogan *et al.*, 2015). These phases have been shown, in turn, to relate to mean westerly low and mid-level winds (Pohl and Camberlin,

2006; Hogan, *et al.* 2015). Berhane and Zaitchik (2014) gives more detail regarding the Congo airmass influence and states that their analysis of daily westerly winds during a rain-enhancing phase of the MJO exhibits few absolute westerly flows during March–May, but several in November–December. One past study has focused directly on the identification of westerly winds and their effect on East Africa (Nakamura, 1968). Unfortunately, we do not have the ability to read the full article which is in Japanese, but a translated abstract makes the broad conclusions of the work clear and we can see that the paper’s figures support the conclusions. Nakamura (1968) does not make the distinction as Berhane and Zaitchik (2014) do between the rainy seasons but the following statements may still be consistent: “frequent appearances of westerlies and their rain-bringing character have long been known”; “pilot balloons and radio-sonde observations show there is a distinct seasonality in the frequency of appearance, with the two minima in April and in November, which are common to most of the stations in East Africa.” Nakamura (1968) highlights, as do Nicholson (1996) and Pohl and Camberlin (2006), that westerlies have different effects on different parts of East Africa: “the Kenya Highlands experience frequent afternoon showers”, while “extreme dry conditions prevail to the east of the East Africa Highlands”. Given that the highlands are closest to the Congo, it is reasonable to think they are most directly affected by the Congo airmass, while the coastal area is part of a rain shadow during prevailing westerlies. Thanks to the broad range of satellite precipitation estimates and reanalysis data now available, it seems appropriate to give new focus to the balance of Congo and Indian Ocean influence on the East African Rift Valley region.

The rain-enhancing phases over the East African highlands are MJO phases 2–4, which are when the MJO convective core is over the Indian Ocean, not Africa, implying the rain-enhancement is an indirect consequence of the MJO convection. The established Matsuno–Gill response of the MJO (Matsuno, 1966; Gill, 1980) includes anomalous westerlies to the west of the MJO convective core, consistent with the anomalous low-level westerlies seen over East Africa. The Matsuno–Gill response also includes anomalous cyclonic activity to the northwest and southwest of the MJO convective core, and therefore it is not surprising that the MJO phases 2–4 are associated with increased likelihood and intensification of tropical cyclone activity in the South Indian Ocean (Bessafi and Wheeler, 2006; Klotzbach, 2014). This connection hints that Indian Ocean tropical cyclones may also play an indirect role in enhanced rainfall over East Africa. The effect would be indirect rather than direct since tropical cyclones cannot form close to the Equator. Tropical cyclones that are remote from East Africa have indeed been proposed as a

key indirect driver of the high rainfall during the 2018 long rains (Kilavi *et al.*, 2018; Mwangi *et al.*, 2018). However, we are not aware that any study has established the combined effects of the MJO, tropical cyclones and westerlies on East African rainfall.

Following the data and methods sections (Sections 2 and 3), we use a case-study of the 2018 long rains (Section 4) to provide context of the interacting influence of westerlies, the MJO and tropical cyclones on East African rainfall. As mentioned, the long rains of 2018 were particularly wet, especially considering the decline in the long rains over the past decades (Kilavi *et al.*, 2018; Mwangi *et al.*, 2018). The aim of analysing the case-study here is to clearly demonstrate the potential role, and interactions, of westerlies within the season. We then move beyond the case-study to study the statistics of the dynamics over multiple decades. In Section 5, 40 years of reanalysis and observed rainfall are used to give the first comprehensive study of how moisture flux from the Congo and Indian Ocean airmasses affect East African rainfall in different seasons. Section 5 also looks more closely at variability of the long rains, since the recent drying trend has had damaging impacts on East African communities. Finally, Sections 6 and 7 look at how westerlies during the long rains are related to the larger-scale atmospheric features of the MJO and cyclonic activity in the Indian Ocean.

2 | DATA

Two rainfall observational products are used: the Global Precipitation Climatology Project (GPCP; Adler *et al.* 2003) and the Climate Hazards Group InfraRed Precipitation with Station data (CHIRPS; Funk *et al.*, 2015). Both products use satellite precipitation estimates along with rain-gauge observations. CHIRPS uses predominantly infrared-based estimates, while GPCP uses infrared- and microwave-based estimates. GPCP provides global 2.5°, monthly data from January 1979 to the near present. Daily GPCP data are available for years since 1998. CHIRPS provides daily 0.05° rainfall data between 50°S and 50°N since 1981. Both datasets provide full coverage over the African continent. Maidment *et al.* (2015) found that, compared to other rainfall datasets, both the GPCP and CHIRPS datasets have relatively small deviations from the Climatic Research Unit rainfall data over Africa. In this study, the GPCP dataset is mainly used to study interannual variability of the long rains, whilst CHIRPS is used to study the relationship between daily moisture flux and rainfall.

The European Centre for Medium-Range Weather Forecasts (ECMWF) Interim Re-Analysis (ERA-Interim; Dee *et al.*, 2011) is used to study the meteorological conditions associated with East African rainfall. Diagnostics

used are vertically integrated eastward and northward water vapour fluxes, mean sea level pressure, total precipitation, relative vorticity, surface pressure, and zonal wind, relative humidity and specific humidity on pressure levels. All data are used on a 0.75° grid and averaged to daily means from 6-hourly data (or accumulations from 12-hourly data in the case of precipitation). The vertically integrated water vapour flux variables are available directly from ECMWF. The majority of atmospheric moisture is in the form of water vapour so we shorten the term to "moisture flux". The eastward and northward moisture flux variables are calculated as the integral, over all model levels, of the product of water vapour, the eastward or northward wind, and the vertical pressure difference across the model level. The integral is then divided by the gravitational acceleration constant, resulting in units for the moisture flux variables of $\text{kg}\cdot\text{m}^{-1}\cdot\text{s}^{-1}$.

Daily MJO indices from the Bureau of Meteorology are used (<http://www.bom.gov.au/climate/mjo/>, accessed 14 November 2019). These are calculated using a pair of empirical orthogonal functions of interpolated NOAA outgoing long-wave radiation (OLR) satellite observations (Liebmann and Smith, 1996) and reanalysis winds at 850 and 200 hPa following Wheeler and Hendon (2004). The corresponding principal components, of which there are two, are referred to as the Real-time Multivariate MJO series 1 and 2. The amplitude and phase of these principal components can be used to represent the MJO. Where the amplitude is less than 1, we define this as an inactive MJO.

Locations and times of tropical cyclones in the north and south Indian Ocean have been obtained from the International Best Track Archive for Climate Stewardship (IBTrACS) best-track version 3 (Levinson *et al.*, 2010). IBTrACS combines the tropical cyclone best track data from all forecasting agencies into an integrated dataset. Reports in the dataset are on a 6-hourly frequency. The analysis of tropical cyclones here only uses the March–May season. All tracks in the dataset have been used in our analysis regardless of intensity. This means any storm ranging from tropical disturbance to category 5 tropical cyclone is included. We have included all storms since all will be off-Equator, low pressure systems potentially exhibiting some degree of rotation favourable to westerlies along the Equator and therefore may have a remote influence upon East Africa. Analysis of a sub-selection of storms which reached tropical depression strength (maximum sustained wind of 34 kts) supports the conclusions based on the full dataset used in this paper. The World Meteorological Organisation (WMO) version of the dataset is used, which provides tracks up to 2016, and uses the data from the WMO-sanctioned ocean basin Regional Specialized Meteorological Centres and Tropical Cyclone Warning Centres.

For the Indian Ocean these centres are: La Réunion, New Delhi and the Australian Bureau of Meteorology.

3 | IDENTIFICATION OF THE FOCUS REGION AND AIRMASS EFFECTS

Our focus region is shown as the box on Figure 1a, and could be described as an expanded Lake Victoria Basin region, or a subregion of the East African Rift Valley. As discussed by Nicholson (2017), “East Africa” is often used to formally refer to Kenya, Uganda and Tanzania. Since our region includes significant portions of these countries, we use the term “East Africa” throughout the paper for brevity when referring to the study region. The region chosen does not fully encompass these countries because we have focused on the region with biannual rainfall whilst excluding coastal areas. Coastal areas of Kenya and Tanzania, and other bimodal rainfall regions in the Greater Horn of Africa, have been excluded because the atmospheric dynamics involved in these regions differ from those around Lake Victoria (Nicholson, 2017). Notably, they are lowland areas with close proximity to the Indian Ocean and which experience the strong low-level Somali jet, which is not present in the highlands. It has been noted many times that westerlies affect coastal locations differently to the East African Rift Valley (Nakamura, 1968; Nicholson, 1996; Pohl and Camberlin, 2006). Finally, most of the focus region experienced its wettest long rains on record in 2018, which has been identified as being influenced by westerlies, the MJO and tropical cyclones (Kilavi *et al.*, 2018), and is therefore of interest to this study.

To define the airmass influencing this region of East Africa we take an average of the vertically integrated westerly moisture flux over an East Africa box (Figure 1a). When this value is positive we consider the region to be influenced by the Congo airmass, and when it is negative the region is influenced by the Indian Ocean airmass. We also split the days with negative values into strong and weak as we find these have different responses, and this aids interpretation in relation to westerly anomalies presented in the literature.

If there is curvature of moisture fluxes from a southerly or northerly flow, then the above metric may not precisely represent the airmasses proposed. Therefore, we have also performed analysis using a metric of the vertically integrated westerly moisture flux through the western edge of the East Africa box (Figure 1a). This ensures that there is either a westerly flux in from the Congo or not, which is our primary interest in this investigation. No additional analysis has been undertaken to also establish the effect of northerly or southerly components of the flow. The zonal

flow into and across East Africa is the focus. Results and conclusions with this edge method are similar to those with the box-average method so we generally do not show results with this metric. However, where notable differences exist, these are mentioned in the text.

4 | CASE-STUDY OF 2018 LONG RAINS

A report on flooding in Kenya during the 2018 long rains said “The heavy rainfall has caused flooding, landslides, loss of property and life in some parts of the country” (Mwangi *et al.*, 2018). Kilavi *et al.* (2018) report that “Over the Kenya-core region and indeed Kenya as a whole, 2018 saw the wettest MAM season over the 119-year record of the Global Precipitation Climatology Centre (GPCP) data, and the 118 years of Centennial Trends (CenTrends) data.” Their figure 2c shows that this was in fact the case for the majority of the Lake Victoria Basin. The influence of westerlies, the MJO and remote tropical cyclones was noted, and therefore this case-study provides an opportunity for us to look at the interaction of these features in more detail.

Kilavi *et al.* (2018) also described that this heavy rainfall season had many serious impacts, including an estimated 186 flood-related deaths, approximately 300,000 flood-displaced people, and disruption to schools affecting more than 100,000 students. These impacts starkly show that the rains of 2018 had many destructive results in Kenya, and provide further motivation to understand the controls on the events during March–May 2018. Although Kilavi *et al.* (2018) identify the coincidence of remote tropical cyclones, the MJO, anomalous westerlies, with the enhanced rainfall of 2018, the remainder of their study focuses on evaluation of forecast skill for the season. Therefore, we begin our study with complimentary analysis of the 2018 long rains, in order to motivate further study of the recent history of East African long rains and influence of the Congo airmass.

Figure 1 shows the 2018 long rains anomaly in the GPCP dataset, along with time series of rainfall and westerly moisture flux in ERA-Interim, and number of days spent in significant MJO phases from the NOAA dataset. The observed rainfall anomaly (Figure 1b) shows that rainfall was particularly enhanced over all of Eastern Africa and the western Indian Ocean during the 2018 long rains. We also note dry anomalies over the Sahara and eastern equatorial Atlantic. The dryness in these locations may relate to circulation changes affecting East Africa, but we do not analyse them further here. The East Africa region was the only tropical land region that year to deviate far from the climatological average rainfall (not shown). We have chosen to focus on a region around Lake Victoria and

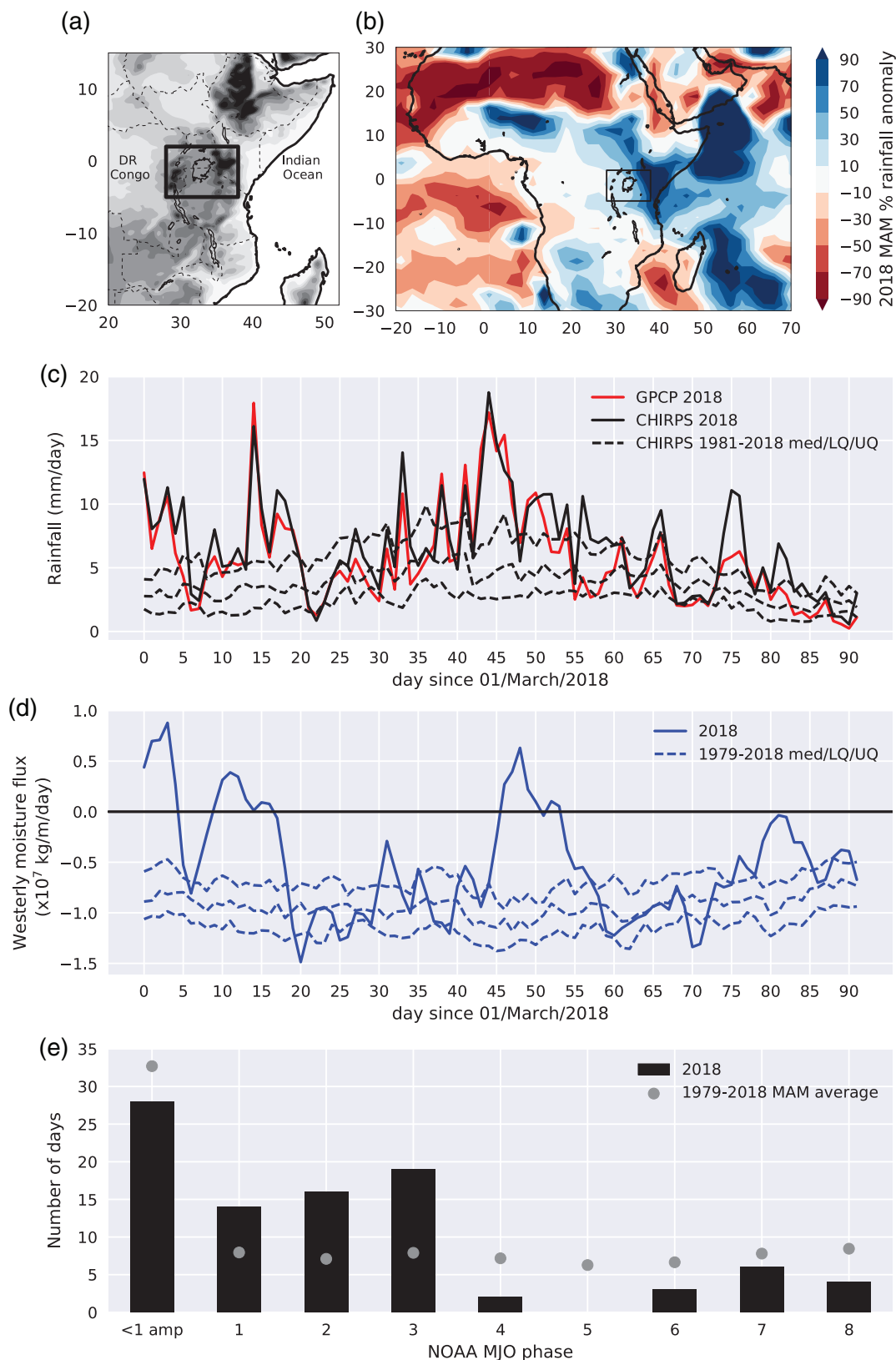


FIGURE 1 Summary of rainfall, ERA-Interim column-integrated westerly moisture flux and MJO during the 2018 East Africa long rains. The box in (a) shows East Africa region of study, and the averaging region for time series in (c) and (d), where dotted lines show the medians (med), lower quartiles (LQ) and upper quartiles (UQ) calculated using data within the range of years listed in the figure legends. (b) shows the anomaly of March–May 2018 rainfall, and (e) shows the number of days in March–May within each MJO phase.

the East Africa Rift Valley for further analysis (Figure 1a, Section 3). This region sits adjacent to the Congo region and showed widespread enhanced rainfall (10% to 90%+) during the 2018 long rains.

Figure 1c shows rainfall time series for the East Africa box in Figure 1a from CHIRPS and GPCP, with the 38-year CHIRPS median and lower and upper quartiles included. Both observational datasets show similar peaks which are anomalously high for the time of year. Kilavi *et al.* (2018) have also shown that both these datasets perform well over Kenya during this period compared to gauge station measurements. The three periods where rain rates are anomalous compared to the climatology are: days 0–5 (P1), days 14–19 (P2), and days 43–54 (P3). These three periods broadly match the three periods identified as high rainfall over Kenya by Kilavi *et al.* (2018). Enhanced rainfall at the beginning of the season during P1 and P2 coincide with the presence of cyclones near Madagascar (tropical cyclones *Dumazile* and *Eliakim*). The corresponding westerly moisture flux (Figure 1d) also aligns with those two peaks in rainfall, with a third period of westerly moisture flux during the prolonged April rainfall of P3 which also coincided with a third tropical cyclone (tropical cyclone *Fakir*). We can see that the climatological average moisture flux is generally easterly during this period, suggesting that the westerly air brought from the Congo may have led to the 2018 rainfall enhancement. In addition to the tropical cyclones and anomalously westerly moisture flux, the 2018 long rains were under the influence of phases 2–3 of the MJO cycle for approximately 35 out of the 90 days (Figure 1e). Compared to the average days in each phase (Figure 1e, grey dots), this number is particularly high. During these phases East Africa is known to experience enhanced rainfall conditions over the highlands (Pohl and Camberlin, 2006; Hogan *et al.*, 2015). Furthermore, analysis by Hogan *et al.* (2015) gives an indication that phase 3 tends to be accompanied by anomalous low-level westerlies across East Africa, consistent with the Congo influence presented here. In addition, our work shows there were more days in the 2018 long rains, than in an average year, with an active MJO, i.e., there were more days with amplitude greater than 1. This is consistent with the work of Pohl and Camberlin (2006) and Vellinga and Milton (2018), who identified a correlation between the long rains and seasonal amplitude of the MJO.

We show in Figure 2 that in the case-study of 2018, there is a direct connection between the westerlies in March 2018 and the tropical cyclones *Dumazile* and *Eliakim* passing Madagascar at the same time (seen as low pressure values in top row of Figure 2). We can also see there is coincident rainfall in East Africa on these days. We have described in Section 1 that, in the literature, independent connections are made between the MJO and tropical

cyclones, and between westerlies over East Africa and the MJO. Yet there has so far been no investigation of the combination of all these effects on enhancing East African rainfall. The remainder of this study develops aims to form new understanding of the combination of effects, beginning with the climatology of westerlies in the next section.

5 | CONTRASTING EFFECTS OF AIRMASSES ON RAINFALL

Before exploring the interaction of the Congo Air mass, tropical cyclones and the MJO further, we first characterise the relationship between the moisture flux and East African rainfall using a multi-decade time series of observed rainfall from the CHIRPS and GPCP products, and mean westerly column moisture flux from ERA-Interim. An East Africa region is defined as the box in Figure 1a, and the average of rainfall and moisture flux over that box are taken. The results are separated into days with a westerly moisture flux (i.e., Congo influence), strong easterly moisture flux (Indian Ocean influence), and weak easterly moisture flux. This third category seems to exhibit different characteristics to the strong easterly days, and also would correspond to westerly anomalies in analysis in the literature.

5.1 | Relationship of airmasses to daily rainfall variability

In the 2018 long rains, periods of westerly moisture flux coincided with periods of higher rainfall (Figure 1). Figure 3a shows that for all April days between 1981 and 2018, the days with a westerly flux (blue points) always produce at least some rainfall within the East Africa box shown in Figure 1. Furthermore, it shows that larger easterly moisture fluxes (red points) generally have lower rainfall rates than weaker easterlies ($> -0.5 \times 10^7 \text{ kg} \cdot \text{m}^{-1} \cdot \text{day}^{-1}$) (orange) or westerlies. The divide between strong and weak easterlies is somewhat arbitrary but it serves to demonstrate that it is not a simple distinction between easterlies and westerlies.

For each month, the boxplot distribution for each category is shown in Figure 3b. It shows that across all months the median and upper and lower quartile rain rates of the westerly distributions are higher than the those of strong and weak easterly distributions. The indentations of the boxes around the median show the 95% confidence from bootstrap resampling, and therefore gives a sense of the significance of the difference in medians. In some months (September to November) this confidence interval is wider than the interquartile range because there are

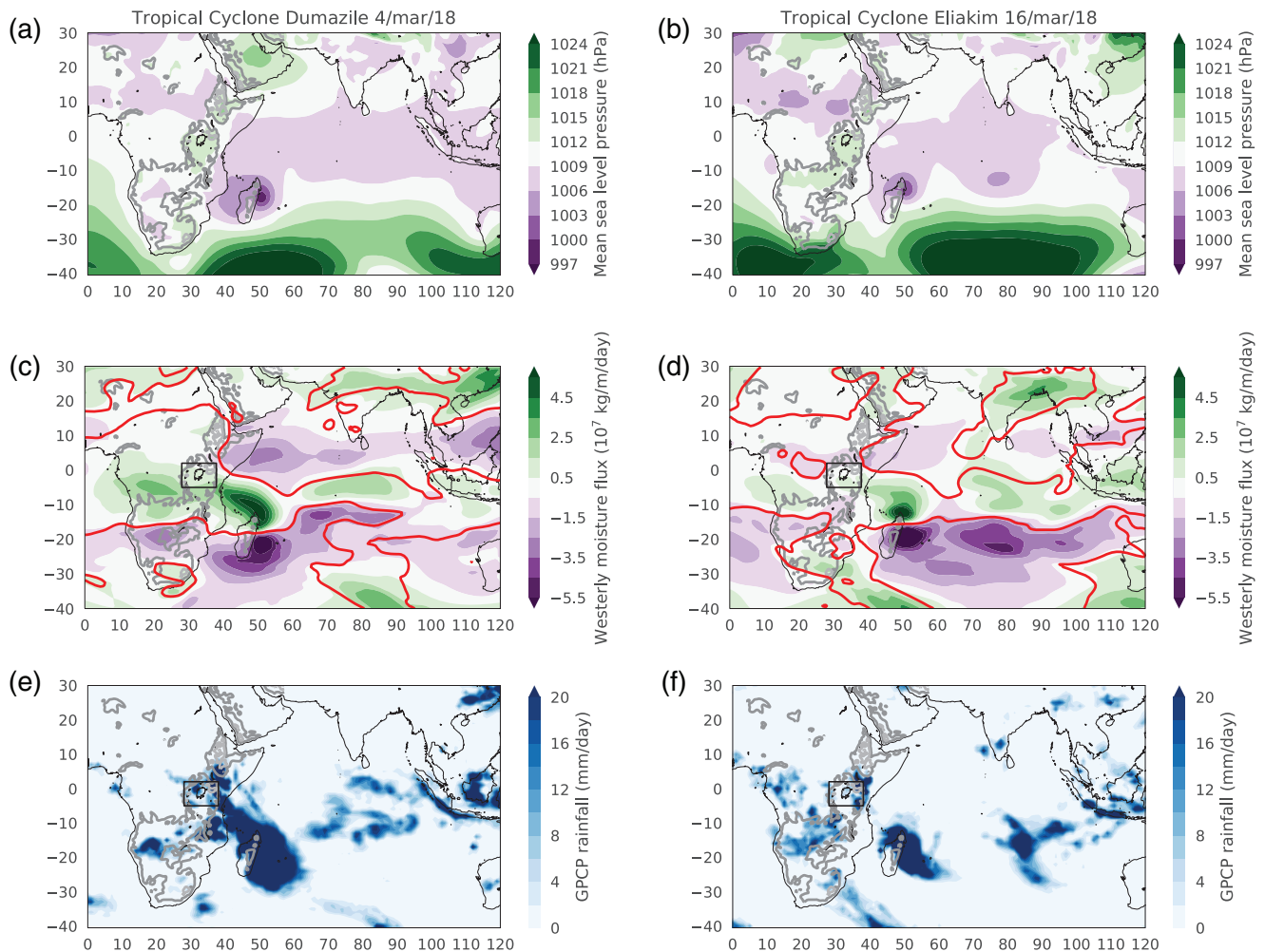


FIGURE 2 (a, b) ERA-Interim mean sea level pressure, (c, d) ERA-Interim column-integrated westerly moisture flux and (e, f) GPCP rainfall on (a, c, e) 4 March 2018, and (b, d, f) 16 March 2018 during which cyclones *Dumazile* and *Eliakim*, respectively, were present to the east of Madagascar. In (c, d) the red line shows the zero contour of westerly moisture flux anomaly compared to the 1979–2018 climatology. Boxes show the East Africa region of study.

few occurrences of westerly moisture flux days in these months. For the months where confidence intervals are better constrained (December to August), the median rain rate on days with a westerly moisture flux is significantly higher than the median on days with a strong easterly moisture flux. Although the medians of westerly days are higher than the medians on weak easterly days for all months, there is overlap of the confidence intervals for some months, suggesting these may not all be significant differences.

As already mentioned, some months have very few occurrences of westerly days. Figure 3c shows the average percentage of all days in each month that have a westerly moisture flux or a weak easterly moisture flux. The occurrence of westerly moisture flux varies from near-zero in the September–November period (encompassing much of the short rains season), to approximately 4% in the long rains (March to May), to up to 11% in the dry seasons. The

minima in April and November are consistent with those found in the study of westerlies by Nakamura (1968), but we find that the long rains have higher occurrence than November–December, which is different to the results of Berhane and Zaitchik (2014). This is possibly due to differences in how westerlies are defined but Berhane and Zaitchik (2014) give few details about this part of their analysis. For our findings, the higher frequency of westerlies in the long rains compared to short rains offers a hypothesis for why short rains are more predictable on a seasonal time-scale (Walker *et al.*, 2019). The formation of westerlies occurs on short, synoptic time-scales. Since there are no known drivers that provide a forecast for such synoptic patterns months in advance, it is not surprising that the season with higher frequency of westerlies is less predictable. The recent work of Vellinga and Milton (2018) using MJO amplitude to explain long rains variability, whilst not directly referring to westerlies, suggests there

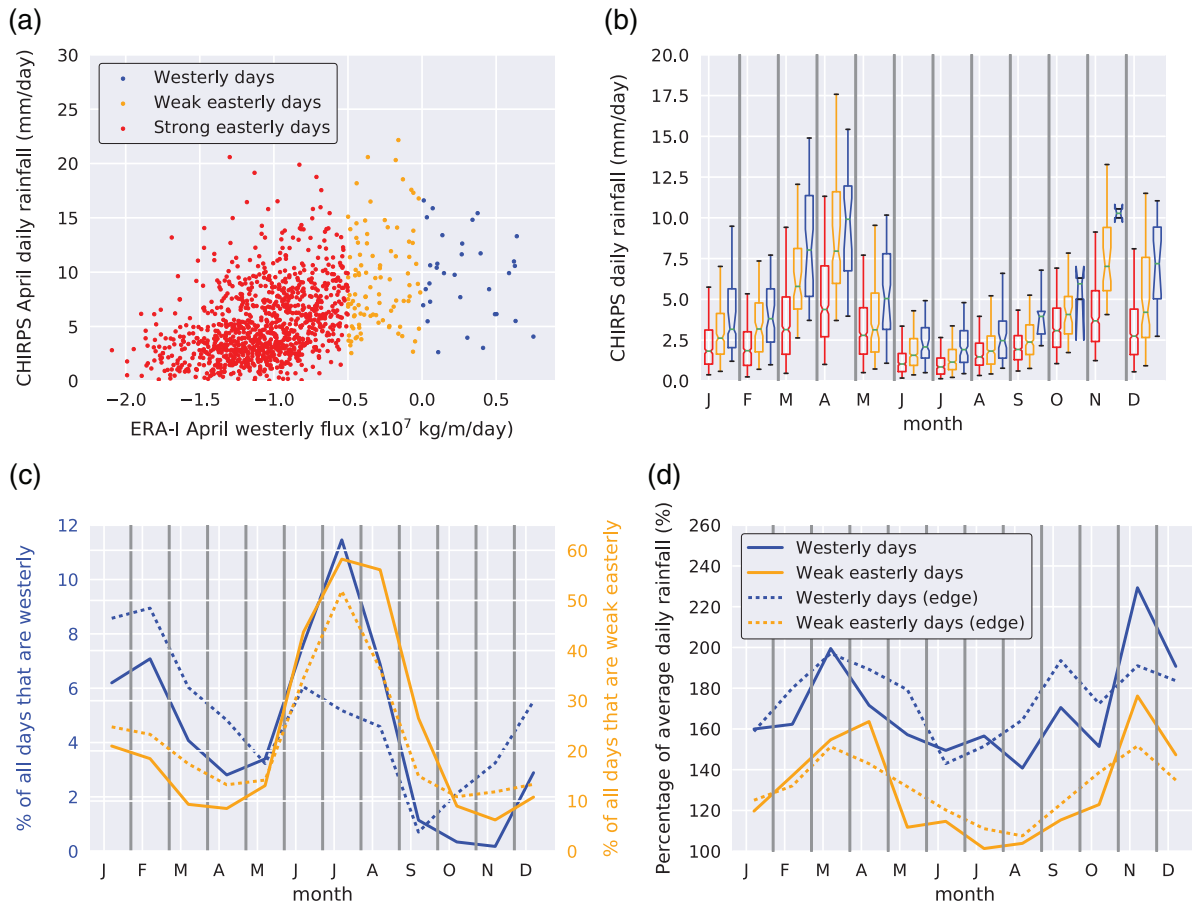


FIGURE 3 Comparison of daily vertically integrated westerly moisture flux and rainfall 1981–2018. (a) Individual daily values for April with westerly moisture flux days (blue), weak easterly days (orange) and strong easterly days (red). (b) Boxplots of rain rates by month and by moisture flux categories in (a). Whiskers show 5th and 95th percentiles. Indentations (notches) of the boxes around box plot medians shows 95% confidence interval calculated from a bootstrap resampling of 1000 values. (c) Average percentage of days in each month with westerly (blue) or weak easterly (orange) moisture flux; note different scales for the two categories. (d) Percentage of all-day mean rain rate for average rain rate on days with westerly (blue) or weak easterly (orange) moisture flux. (a, b) use the area-average method for compositing; results are similar when using the edge method (methods described in Section 3). In (c, d), solid lines show analysis when using the composite based on area-average, while dotted lines show the analysis when using the composite based on the edge method.

may be potential for improving forecast skill using the MJO. However, the challenge in accurately representing the long rains variability remains, since few climate models can satisfactorily reproduce intra-seasonal/synoptic controls such as the MJO. Interestingly, there is not the same distinction between rainy seasons in the number of weak easterly days, pointing specifically towards westerly moisture flow as a potential distinguishing feature between the two seasons.

It is also interesting to see that westerly days are more prevalent in the dry season. Whilst total rainfall during the dry seasons may not have as a great a societal interest as that during the rainy seasons, short-lived intense storms can still cause problems, especially for fishermen on Lake Victoria. Woodhams *et al.* (2019) has shown that a northwesterly wind was present in a case-study of a Lake Victoria storm in July, and provide evidence that it

introduced additional moisture to the storm environment. However, we note that the occurrence of westerly moisture fluxes during June–August dry season is lower when using the western edge method of identification (described in Section 3), closer to 5% of days (Figure 3c). This suggests that there may be curvature of the moisture flux from a northerly or southerly direction in these months. This result is consistent with the fact that the tropical rain band will be located to the north of the region and, on average, a strong southerly component of moisture flux can be expected. All the same, there is evidence here that the Congo airmass has an important influence at many times of the year, even if on a minority of days.

The higher rain rates on these days clearly is an important consideration for daily variability throughout much of the year. Figure 3d quantifies the average enhancement of daily rainfall on westerly and weak easterly days. Westerly

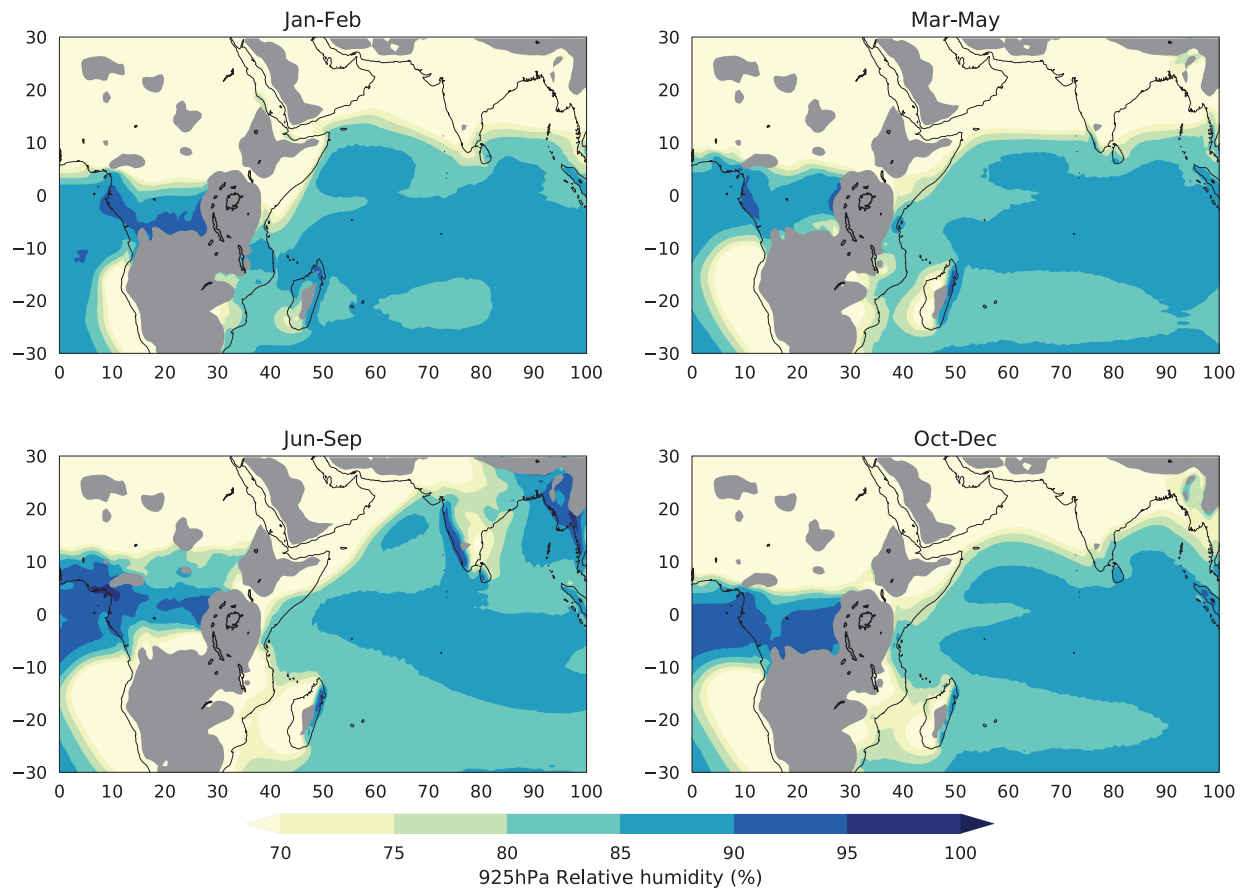


FIGURE 4 Climatological seasonal mean 925 hPa relative humidity in each season from ERA-Interim using 1979–2018. A grey mask is applied over all areas with seasonal average surface pressure less than 925 hPa.

days lead to an increase in average daily rainfall of 40 to 100%, depending on the month and not considering the high November value since there is low sample size in that month. This average enhancement is greater in all months than the enhancement on weak easterly days which show an average enhancement from 0 to 80%. Therefore, despite being in a minority, days with a Congo airmass disproportionately contribute to monthly rainfall accumulations (i.e. at least 40% more than would be expected on average based on the proportion of all days that were westerly).

5.2 | Drivers of the effect of airmasses on rainfall

We now consider possible reasons for the different responses of East African rainfall to the direction of moisture flux. Figure 4 shows seasonal mean relative humidity at 925 hPa. There are general features common across all seasons and therefore may explain the consistent effect of westerlies on rainfall year-round (Figure 3). Over the Congo, and particularly near the border with East Africa, air is at a high relative humidity of 90–95%, already close

to saturation, while to the east of Lake Victoria relative humidity is lower. Over the closest parts of the western Indian Ocean relative humidity is less than 85%, and even lower over land. Meanwhile, weak easterly moisture flux days may lead to higher rainfall because there is less import of lower relative humidity air from the Indian Ocean, and local moisture sources, such as Lake Victoria itself, have a greater influence on available atmospheric moisture in the region.

It is important to consider how the humidity of air relates to the wind, so Figure 5 shows an average vertical profile averaged between 5°S and 2°N (i.e., the latitudinal extent of the East Africa box, Figure 1a) of zonal wind, specific humidity and relative humidity composited for the different categories of moisture flux days. In all categories, there is a deeper layer of high specific and relative humidity air over the Congo than over the Indian Ocean. The figure shows that on easterly days (Figure 5a), which form the majority of days, there is a low-level easterly wind from the Indian Ocean passing over East Africa and into the Congo region. A shallow westerly flow over the western Congo can be seen. These westerlies can also be expected to form in the eastern Congo in

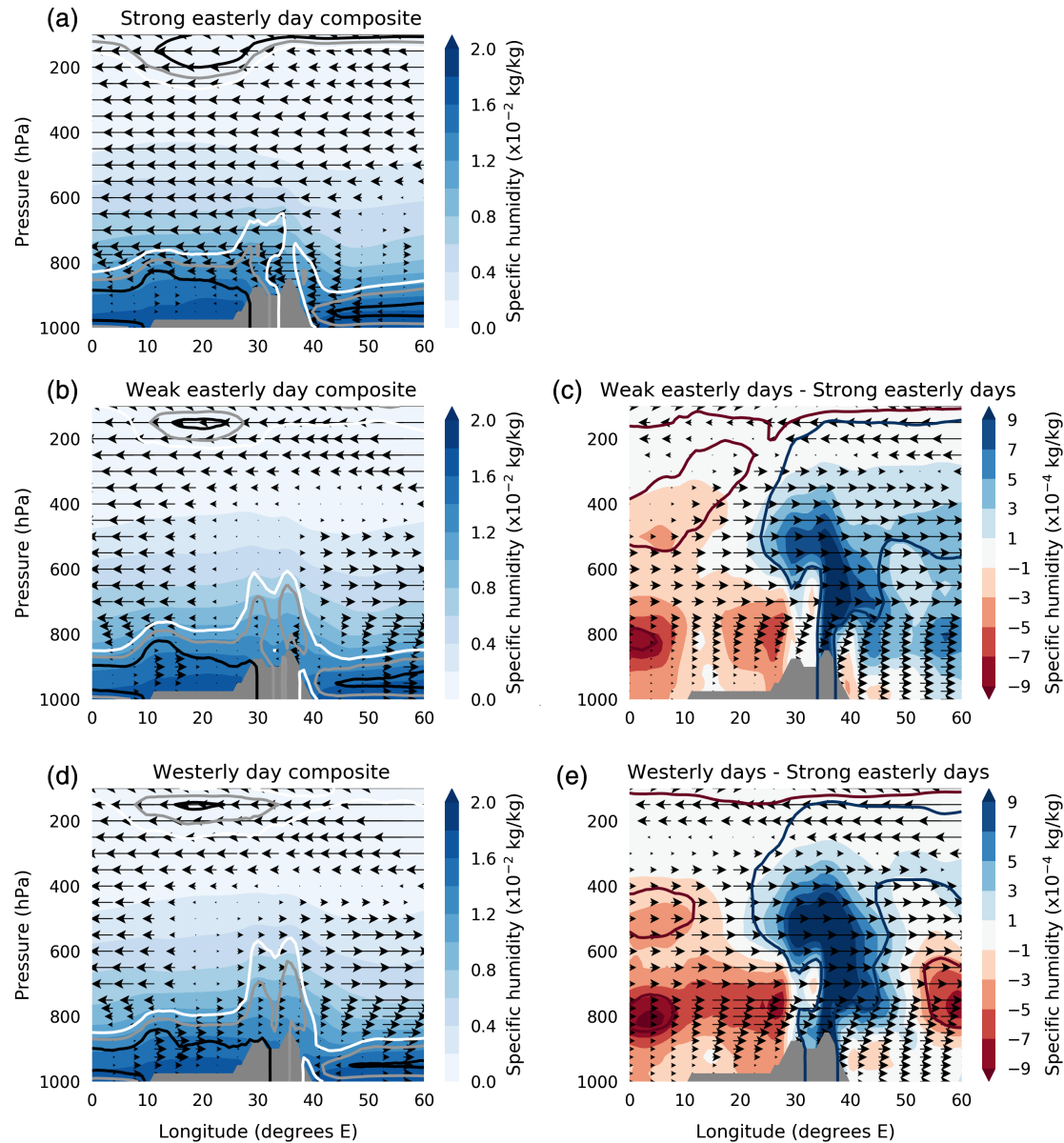


FIGURE 5 Longitude–pressure transects of ERA-Interim specific humidity, relative humidity and zonal wind on pressure levels using days composited by moisture flux categories: (a) strong easterly with moisture flux $< -0.5 \times 10^7 \text{ kg}\cdot\text{m}^{-1}\cdot\text{day}^{-1}$, (b, c) weak easterly with moisture flux $> -0.5 \times 10^7 \text{ kg}\cdot\text{m}^{-1}\cdot\text{day}^{-1}$, and (d, e) westerly. (a, c, d) show mean values and (c, e) show anomalies with respect to the strong easterly day mean shown at (a). In (a, b, d), white, grey and black contours are 75, 80, 85% relative humidity, respectively. In (c, e), dark red and blue contours are -5% and $+5\%$ relative humidity, respectively. Data are used for 1979–2018 for all months. An average over the latitudinal extent of the study region (5°S to 2°N) is used to form the transects. Grey shading masks pressure levels greater than the annual longitudinal mean surface pressure.

the afternoon when afternoon anabatic (upslope) flows generate convergence with the mean easterlies on the mountains of the eastern Congo, and this will also occur on the mountains to the east of the Lake Victoria basin. The relative humidity contours show that on these days relative humidity is low over East Africa. On westerly days (Figure 5d), there is still a shallow low-level easterly from the Indian Ocean, but this is accompanied by a deep layer of low-level westerlies across the Congo basin and across

East Africa. These westerlies converge with the low-level easterlies from the Indian Ocean on mountains to the east of Lake Victoria at $35^\circ\text{--}40^\circ\text{E}$. We can see in Figure 2 examples of how the location of this convergence likely drives rainfall over those mountains. Therefore, as well as bringing high relative humidity air, the westerlies drive mean convergence in East Africa which supports the afternoon occurrence of anabatic flows. The westerlies at mid-levels and over the Indian Ocean show that the occurrence of

westerlies across East Africa is a large-scale feature of the atmosphere. We note in the anomaly plot (Figure 5e) that there is an increase of humidity at upper levels over East Africa as a result of the convection that occurs, and also a reduction in specific humidity over the Congo region. This is consistent with reduced convergence on the eastern Congo mountains, and a reduced likelihood of storm formation. We note that similar patterns exist on weak easterly days (Figure 5b,c), but that the enhancements to convergence in the mean flow and relative humidity are smaller than on westerly days. One notable difference between Figure 5c,e are the mid-level (800–600 hPa) humidity differences between 50° and 60°E. This appears to be a region of divergence in the surface to mid-level flow (Figure 5a,b,d) which will result in subsidence and drawing down of dry upper-level air. The differences highlight an association during westerly flow between stronger convection over East Africa and stronger subsidence over the neighbouring Indian Ocean.

Using the edge method of westerly identification (described in Section 3) exhibits some differences in these composites (not shown). With the edge method analysis, along with the deep layer of low-level westerlies, there is also a deep layer of low-level easterlies, and therefore this method is identifying days where there is strong convergence of winds, and less with the dominance of one air mass or other on a particular day. This is a key reason we have chosen the area-average method for identifying the days with different airmass influences.

5.3 | Relationship of airmass influence and long rains interannual variability

Having demonstrated the dependence of East African rainfall on the Congo and Indian Ocean airmasses on shorter time-scales, next our analysis considers whether, despite being a minority of days, interannual variability of westerlies and weak easterlies have impacts on longer-time-scale variability of East African rainfall. The focus will be on the long rains (March–May) since this is a season on which people depend to deliver rainfall for agriculture and other needs, as well as the rainy season for which there is the least predictability and understanding. We have not focused here on the short rains season (October–December) because it was shown in Figure 3 that occurrence of westerlies is much lower than in the long rains season.

The time series of long rains anomaly from GPCP is shown in Figure 6a. The dryness of the most recent decade is apparent in the GPCP dataset, with 2018 being anomalous and the highest rainfall in the GPCP time series for this region. In Figure 6b we show stacked bar plots of the

number of days in each year with westerly (blue), weak easterly (orange) and strong easterly (red) moisture flux across East Africa, with the sum adding up to 92 days for each long rains. It is clear that the majority of days each year experience a strong easterly flow from the Indian Ocean. Then there is large year-to-year variability of the number of westerly and weak easterly days. In the recent dry period from 2007 to 2017 there were very few days with a Congo influence, whereas 2018 and other wet years had more days with a westerly moisture flux. To some extent the same can be said for weak easterly days.

In Figure 6c–e we show the GPCP anomaly of Figure 6a against the number of days in each moisture flux category. We can see that the seven years with the highest number of westerly days all had a wet anomaly. Blue crosses show these same years on the other plots and they span a wide range of numbers of weak easterly days, demonstrating that years with a strong Congo influence are discernible from those that have increased weak easterlies. The strong easterlies scatter plot shows that these same years have fewer days with an Indian Ocean influence. Therefore, we conclude that the interannual variability in number of days with a Congo influence is an important factor in understanding the variability of the long rains.

6 | LARGE-SCALE ATMOSPHERIC FEATURES ASSOCIATED WITH THE CONGO AIRMASS DURING THE LONG RAINS

As illustrated in Section 4 and described by Kilavi *et al.* (2018) and Mwangi *et al.* (2018), there are large-scale and remote features of the atmosphere that possibly generate, but at least coexist with, a westerly moisture flux over East Africa. This section investigates such features during the long rains. Figure 7a–d show the average difference between westerly and easterly days for four atmospheric variables. The westerly days make up only a small fraction of all days but there are enough to form a representative average (127 of 3680 days), and these are spread throughout the time series, as can be seen in the distribution of peak westerly years in the time series of Figure 6b.

The variable shown in Figure 7a is the column-integrated westerly moisture flux. This shows that the anomalous westerly moisture flux experienced over East Africa is not a localised feature, but may often be present out to the Atlantic or to the east of the Indian Ocean. The second variable shows ERA-Interim rainfall and confirms that on average the East African Rift Valley has enhanced rainfall when westerlies occur over the region. It also shows that the Turkana channel exhibits a similar response, but that the Kenya/Tanzania coastline,

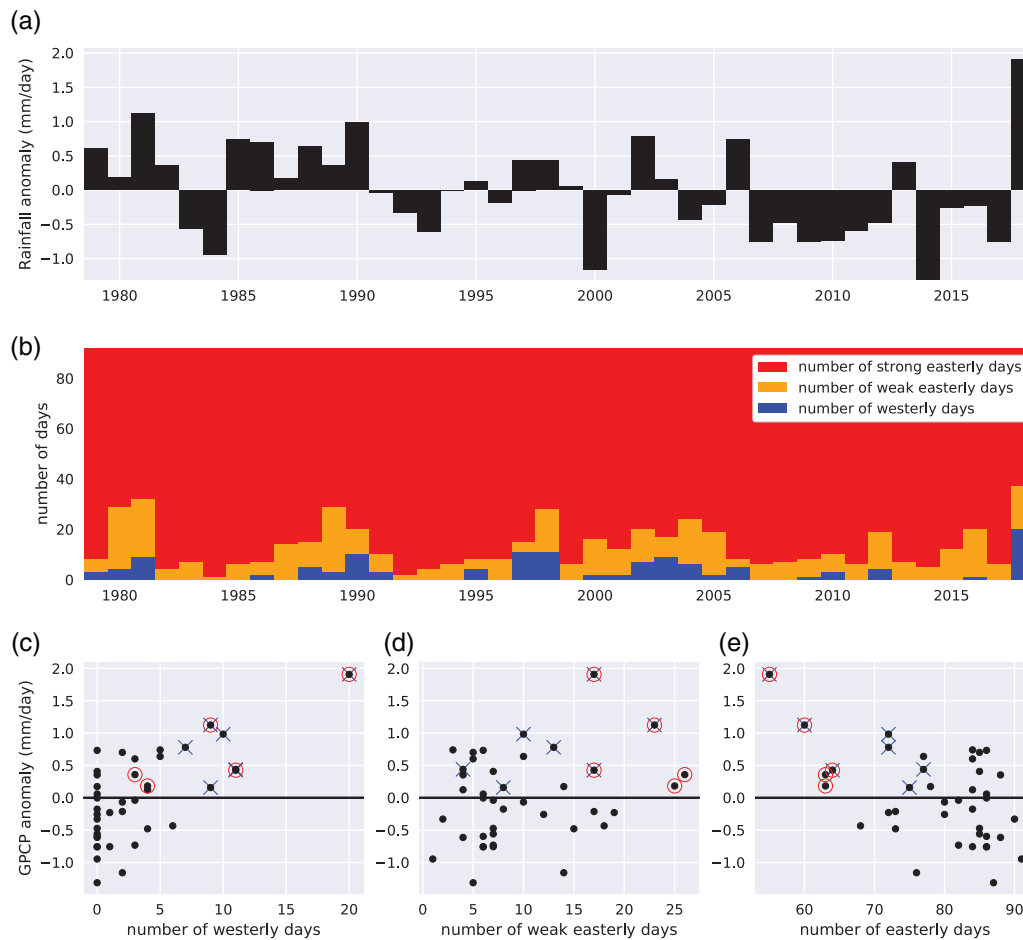


FIGURE 6 East Africa long rains rainfall against number of days in each moisture flux category, using averages over East Africa study region. (a) shows GPCP long rains (March to May) anomaly. (b) shows stacked bar plots of number of days with each moisture flux category present: westerly moisture flux days (blue), weak easterly days with moisture flux $> -0.5 \times 10^7 \text{ kg} \cdot \text{m}^{-1} \cdot \text{day}^{-1}$ (orange) and strong easterly days with moisture flux $< -0.5 \times 10^7 \text{ kg} \cdot \text{m}^{-1} \cdot \text{day}^{-1}$ (red). (c, d, e) For each moisture flux category, GPCP anomaly against number of days with given moisture flux. Blue crosses highlight years with higher number of westerly days and a positive GPCP anomaly. Red circles highlight years with lower number of strong easterly days and a positive GPCP anomaly. In (c) note there are two almost indistinguishable points at $x = 11, y \sim 0.45$.

and the Congo basin itself, have depressed rainfall on these days. The westerly anomalies in the Turkana channel suggest a weaker Turkana jet, and the enhanced rainfall in these conditions is consistent with recent work by Vizzy and Cook (2019). Meanwhile, the depression of rainfall along the coastline during westerlies is consistent with conclusions in the literature (Nakamura, 1968; Nicholson, 1996; Pohl and Camberlin, 2006). The effect can be expected because coastal regions are different from the highlands in that they are affected by the sea breeze, and also that they sit on the lee side (rain shadow) of the highlands during a westerly flow. The third variable in Figure 7 is mean sea level pressure (Figure 7c) which shows on average anomalously high pressure over the African continent, and anomalously low pressure over the Indian Ocean, particularly around Madagascar, and towards the Southern Ocean off the coast of Australia. Again this feature shows

consistent sign of anomalies across a very large area, and suggests the drivers of the westerlies over East Africa are generally remote and large-scale. The deeper low pressure anomalies around Madagascar are a consequence of either more frequent or intense tropical cyclones and/or a weakened Mascarene High. Finally, Figure 7d shows that on westerly days there is anomalously high cyclonic relative vorticity in the Indian Ocean just south of the Equator, consistent with the presence of tropical cyclones.

7 | ROLE OF THE MJO AND TROPICAL CYCLONES DURING THE LONG RAINS

To begin to understand the effect of the MJO and tropical cyclones on the moisture flux across East Africa during

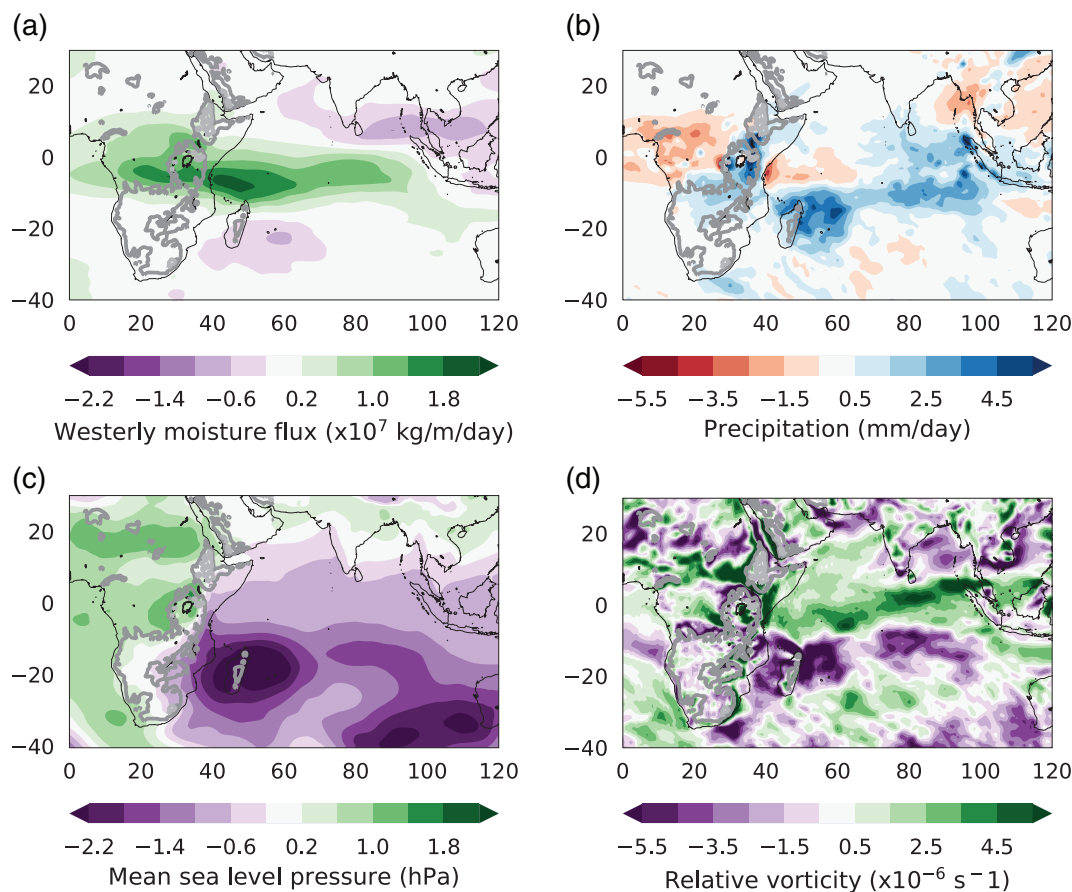


FIGURE 7 Mean difference of atmospheric state on days with westerly moisture flux compared to days with an easterly flux. ERA-Interim variables considered are: (a) column-integrated westerly moisture flux, (b) precipitation, (c) mean sea level pressure and (d) relative vorticity. Note that relative vorticity is positive for cyclonic activity in the Northern Hemisphere, and negative for cyclonic activity in the Southern Hemisphere.

the long rains, we first consider the joint probability distribution of both aspects in Figure 8a. This figure shows the percentage of all days that occurs in each combination of conditions. The most common occurring case is days without a significant MJO and without a cyclone present. We can see that when there is a significant MJO in phases 3 to 5 there is more likely to be a cyclone than not. But this is not the case for other phases of the MJO, thereby consistent with findings by Klotzbach (2014). The equivalent distribution can be produced for westerly days only. The difference of the two distributions (Figure 8b) shows in what conditions westerly days are more likely (positive values) to occur than would be expected based on the all-day probability (Figure 8a). This shows that westerlies occur more frequently than would be expected in phases 3 and 4, and also are more likely in these phases when a cyclone is present. There is no evidence here that tropical cyclones independently increase the chance of westerlies forming, since there are no increased probabilities on days with an inactive MJO (independent of number of cyclones). Altogether these results show that MJO phases 3 and 4 increase

the likelihood of westerlies occurring, and this chance is increased in the presence of one or more cyclones, which are themselves more likely in these MJO phases.

The percentage of days in each moisture flux category associated with MJO conditions are shown in Figure 8c, and associated with tropical cyclones in Figure 8d. The black lines for all days are equivalent to a sum through one axis on Figure 8a. Broadly speaking the probability of an easterly moisture flux day for a given MJO phase follows the all-day probability. Westerlies are less likely to occur on days with an inactive MJO and no cyclone, and more likely in the phases 3 to 4 of the MJO and when there is one or more cyclones present in the Indian Ocean. Figures 8e and f confirm that, in all conditions where confidence intervals on the median are reasonably well constrained, westerlies are associated with higher rain rates than easterly days, with weak easterlies generally showing smaller rain rates but not necessarily significantly different medians from westerly days. However, it is important to acknowledge that there is a response in the rain rates of easterly days to the phase of MJO, i.e. slightly higher

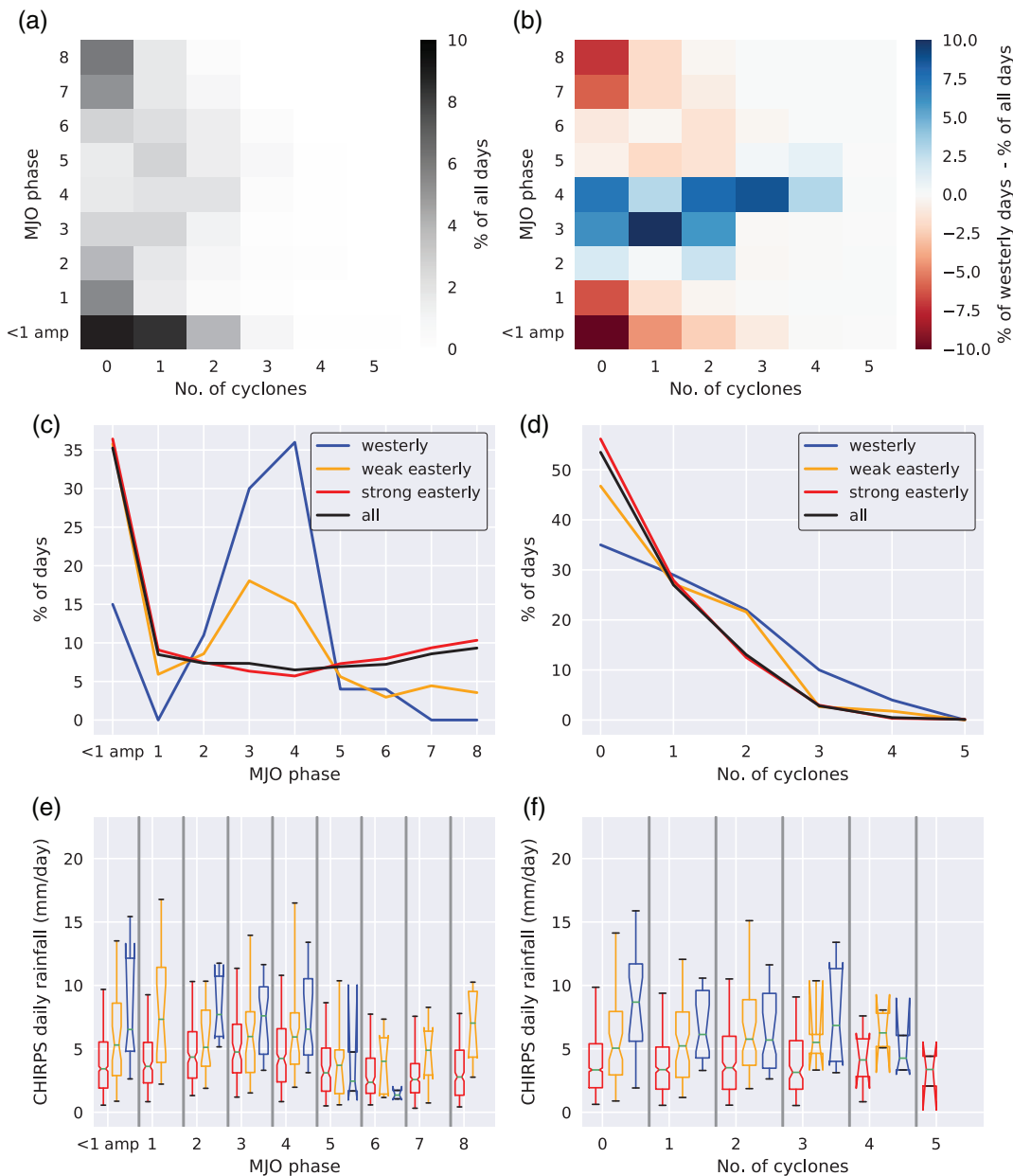


FIGURE 8 Joint density distribution of days occurring in combinations of MJO phase and varying numbers of cyclones during the long rains (March–May). (a) Joint density for all days, (b) difference in joint density distribution for westerly days compared to all days, (c) percentage of days in each moisture flux category by MJO phase, (d) percentage of days in each moisture flux category by number of cyclones. (e, f) are boxplots of rain rates as in Figure 3 but by MJO phase and number of cyclones instead of month. Data for 1979 to 2016 are used. For the tropical cyclone data all tracks from the whole North and South Indian Ocean basins are included.

rain rates in phases 2 to 4. This suggests that, while the enhanced occurrence of westerlies in these phases will be one way in which rainfall could be enhanced, there may be other factors also at play that can enhance rain rates.

Results here support the conclusion that during the long rains there is a connection between the MJO, tropical cyclones, westerly moisture flux from the Congo into East Africa and enhanced rainfall in East Africa. As presented in the introduction, studies have made the connections between individual components of this mechanism but to

our knowledge this is the first paper to demonstrate the interconnection of all components together.

Figure 9 provides one final piece of information relevant to the effect of tropical cyclones. In Figure 9a is shown the percentage of all IBTrACS cyclone locations (up to four reports per day) that occur in each part of the Indian Ocean over the period 1979 to 2016 during the long rains. This shows that the majority of tropical cyclones occur in the southern Indian Ocean. Figure 9b shows the percentage of cyclone locations in each region

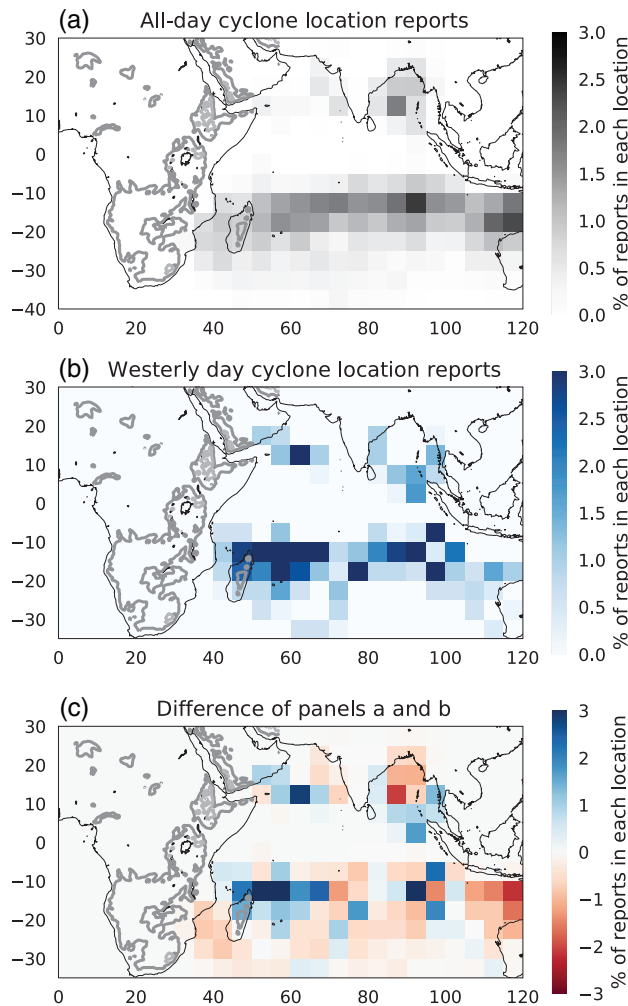


FIGURE 9 Probability density distribution (percentage of reports in each location) of cyclone reports on (a) all days and (b) westerly days during the long rains (March–May). (c) shows the difference between (a) and (b). Locations are based on the location of reports in the IBTrACS dataset which can be up to four per day. Data are used for 1979 to 2016 and for the whole North and South Indian Ocean basins.

on days with a westerly moisture flux across East Africa, and the difference shown in Figure 9c highlights that there is increased likelihood of westerlies when tropical cyclones are located near northeast Madagascar, whereas westerlies are less likely if tropical cyclones are located in the channel between Madagascar and Mozambique. This is consistent with the experiences of 2018 tropical cyclones which did not form in the Mozambique channel and were associated with westerlies across East Africa (Mwangi *et al.* 2018; Kilavi *et al.*, 2018), as well as with the dryness experienced in East Africa as a result of tropical cyclone *Idai* occurring in the Mozambique channel in March 2019 (Daily Active Kenya, 2019). This final result shows that the effect of tropical cyclones is dependent on their location. Potentially there are also differing responses to cyclones

of rainfall across Eastern Africa, with Shanko and Camberlin (1998) having previously shown that Ethiopia can experience drought conditions when cyclones are present in the southwest Indian Ocean. The intensity and structure of tropical cyclones is likely to be important, but it is beyond the scope of this paper to investigate the storms in that detail. Furthermore, in the analysis of Figure 8 which has not distinguished by location, the effect of some single tropical cyclones may be masked. Future detailed study of individual tropical cyclone cases and their effects over East Africa is warranted.

8 | CONCLUSIONS

We have shown that the very wet East Africa long rains of 2018 showed enhanced rainfall associated with westerly moisture flux from the Congo airmass and Indian Ocean tropical cyclones, alongside the presence of MJO phases favourable for enhanced rainfall (Figures 1 and 2). This season inspired our focused study on the role of air masses in East Africa and the combined effects of westerlies, the MJO and cyclones. We draw the following conclusions:

1. The direction of moisture flow across the East Africa region affects the likely rain rates (Figure 3). Strong easterly flow bringing the Indian Ocean airmass tends to lead to drier conditions, whilst westerly flow with the Congo airmass tends to lead to wetter conditions (an average 40% (August) to 100% (March) enhancement of daily rainfall). On days when the prevailing easterly moisture flux weakens, we find that there is also an enhancing of rain rates, but this is smaller than the effect of westerlies (0% (July) to 80% (November)).
2. Days with a westerly flow are much less frequent than those with an easterly flow, ranging from very few days during September–November, to around 4% of all days in March–May, to generally more days in the dry seasons (Figure 3b). The higher occurrence of westerly days in March–May than in September–November may be one factor making it more difficult to provide seasonal forecasts for the March–May season since it suggests Indian Ocean temperatures, which have predictability on longer time-scales, may play less of a role.
3. We show that, year-round, higher humidity over the Congo than over the Indian Ocean is a likely driver of enhanced rainfall during westerlies (Figure 4). Low-level westerlies converging with low-level easterlies on these days is also likely to enhance the formation of storms (Figure 5).

4. There is a relationship between long-rains rainfall and the number of days spent influenced by different air-masses (Figure 6). The relationship is positive with increased westerly or weak easterly days, and negative with increased strong easterly days. 2018 stands out as a year with particularly high number of westerly and weak easterly days, whereas the preceding dry period (2006–2017) has generally little westerly influence.
5. Westerly days are associated with large-scale westerly flow beyond East Africa, and with dry anomalies along the coastline of East Africa and over the Congo (Figure 7a,b). There are low pressure anomalies, particularly around Madagascar and the south-east Indian Ocean, that coincide with cyclonic anomalies, and highlight the coincidence of westerlies with tropical cyclones and/or a weakened Mascarene High (Figure 7c,d).
6. A study of the occurrence of westerly days by phase and number of cyclones shows that westerlies are particularly likely in MJO phases 3 and 4 and with one or more cyclones present in the Indian Ocean (Figure 8).
7. The location of tropical cyclones relates to whether there is occurrence of westerlies across East Africa (Figure 9). Tropical cyclones to the east of Madagascar are associated with the largest enhancement of probability of westerlies forming over East Africa, and notably, to the west of Madagascar, westerly moisture fluxes across East Africa become less likely. This distinction is consistent with some recent tropical cyclone cases in 2018 and 2019 and their influence on East African rainfall.

Research here highlights a key challenge for global climate models and climate projections in that, to represent the variability of the long rains and the weather more generally in East Africa, a good representation of both the MJO and tropical cyclones is needed. Climate models are known to struggle with both aspects. However, there is a reasonable chance these atmospheric features will change with climate change. For instance, intense tropical cyclones are expected to occur more frequently as sea surface temperatures increase (Knutson *et al.*, 2010; Walsh *et al.*, 2016). In addition, even the simulation of current climate is challenging because the flow of moisture from the Congo is affected by the complex orography in the region. For instance, recent work using a high-resolution, convection-permitting climate model has shown a reduced flow of moisture across East Africa into the Congo when compared to a coarser, parametrized-convection model (Finney *et al.* 2019).

There is much possible further work that would build on the findings here, including:

- consideration of lagged effects of westerlies, MJO and tropical cyclones (similar to the Vellinga and Milton 2018 study of MJO amplitude);
- investigation of the role of the meridional component of moisture flux;
- the influence of Rossby and Kelvin waves on formation of tropical cyclones (Bessafi and Wheeler, 2006), and of Kelvin waves on East African rainfall (Jackson *et al.* 2019);
- detailed investigation of tropical cyclone effects on East Africa which will undoubtedly depend on the intensity, development and location of the cyclones, as well as interactions of the cyclones with the prevailing conditions.

This final point would benefit from a detailed investigation of case-studies.


In summary, our results provide new understanding of air-mass influence on East Africa, which plays a role on daily to climate time-scales. Also shown is a new association between variability of the long rains and the number of days with Congo influence in East Africa. Finally, combined effects of MJOs and tropical cyclones are presented. Overall, we provide new insights into key mechanisms affecting East African rainfall over multiple time-scales in order to enable better predictability of rainfall over these time-scales.

ACKNOWLEDGEMENTS

DLF and JHM were supported by the Natural Environment Research Council/Department for International Development (NERC/DFID, NE/M02038X/1) via the Future Climate for Africa (FCFA) funded project, Integrating Hydro-Climate Science into Policy Decisions for Climate-Resilient Infrastructure and Livelihoods in East Africa (HyCRISTAL). JHM was also supported by the National Centre for Atmospheric Science via the NERC/GCRF programme ACREW: Atmospheric hazard in developing Countries: Risk assessment and Early Warning. CEB, BJW and JHM were supported by the UK Research and Innovation as part of the Global Challenges Research Fund (GCRF, NE/P021077/1) under the African Science for Weather Information and Forecasting Techniques (African-SWIFT) project. LSJ was funded under the FCFA project Improving Model Processes for African Climate (IMPALA, NE/MO17176/1) and FCFA project, African Monsoon Multidisciplinary Analysis 2050 (AMMA2050, NE/M020126/1). SW was supported by a Natural Environment Research Council (NERC) industrial CASE award with the UK Met Office (NE/N008227/1). BJW was supported by the NERC SPHERES DTP (NE/L002574/1). Funding for SH came from the Weather

and Climate Science for Service Partnership (WCSSP) Southeast Asia, provided by the Newton Fund. Daily MJO RMM indices were provided by the Bureau of Meteorology at <http://www.bom.gov.au/climate/mjo/> (accessed 14 November 2019). GPCP precipitation data were all provided by the NOAA/OAR/ESRL PSD, Boulder, Colorado, USA, from their website at <https://www.esrl.noaa.gov/psd> (accessed 14 November 2019). Thanks go to Doug Parker for sharing his impressions of regional weather forecasting regarding the importance of tropical cyclones in the 2018 long rains.

ORCID

Declan L. Finney  <https://orcid.org/0000-0002-3334-6935>

Beth J. Woodhams  <https://orcid.org/0000-0003-2070-8279>

REFERENCES

- ACAPS (2018). Kenya Floods, Assessment Capacities Project Briefing Note. Available at: <https://www.acaps.org/country/kenya/special-reports>, accessed 4 June 2019.
- Adler, R.F., Huffman, G.J., Chang, A., Ferraro, R., Xie, P.-P., Janowiak, J., Rudolf, B., Schneider, U., Curtis, S., Bolvin, D., Gruber, A., Susskind, J., Arkin, P. and Nelkin, E. (2003) The version-2 Global Precipitation Climatology Project (GPCP) monthly precipitation analysis (1979–present). *Journal of Hydrometeorology*, 4(6), 1147–1167. [https://doi.org/10.1175/1525-7541\(2003\)004<1147:TVGPCP>2.0.CO;2](https://doi.org/10.1175/1525-7541(2003)004<1147:TVGPCP>2.0.CO;2)
- Anyamba, E.K. (1983). On the monthly mean lower tropospheric circulation and the anomalous circulation during the 1961/1962 floods in East Africa. MSc thesis, University of Nairobi, Kenya. Available at: <http://erepository.uonbi.ac.ke/handle/11295/56834>, accessed 14 November 2019.
- Berhane, F. and Zaitchik, B. (2014) Modulation of daily precipitation over East Africa by the Madden–Julian Oscillation. *Journal of Climate*, 27(15), 6016–6034. <https://doi.org/10.1175/JCLI-D-13-00693.1>
- Bessafi, M. and Wheeler, M.C. (2006) Modulation of South Indian Ocean tropical cyclones by the Madden–Julian Oscillation and convectively coupled equatorial waves. *Monthly Weather Review*, 134(2), 638–656. <https://doi.org/10.1175/MWR3087.1>
- Camberlin, P. and Wairoto, J.G. (1997) Intraseasonal wind anomalies related to wet and dry spells during the "long" and "short" rainy seasons in Kenya. *Theoretical and Applied Climatology*, 58(1–2), 57–69. <https://doi.org/10.1007/BF00867432>
- Daily Active Kenya (2019). Mozambique's cyclone is the cause of Kenya's delayed rains. Available at: <http://dailyactive.info/2019/03/19/weatherman-mozambiques-cyclone-is-the-cause-of-kenyas-delayed-rains/>, accessed 4 June 2019.
- Dee, D.P., Uppala, S., Simmons, A.J., Berrisford, P., Poli, P., Kobayashi, S., Andrae, U., Balmaseda, M., Balsamo, G., Bauer, P., Bechtold, P., Beljaars, A.C.M., van de Berg, L., Bidlot, J., Bormann, N., Delsol, C., Dragani, R., Fuentes, M., Geer, A.J., Haimberger, L., Healy, S.B., Hersbach, H., Hólm, E.V., Isaksen, L., Kållberg, P., Köhler, M., Matricardi, M., McNally, A.P., Monge-Sanz, B.M., Morcrette, J.-J., Park, B.-K., Peubey, C., de Rosnay, P., Tavolato, C., Thépaut, J.-N. and Vitart, F. (2011) The ERA-Interim reanalysis: configuration and performance of the data assimilation system. *Quarterly Journal of the Royal Meteorological Society*, 137, 553–597. <https://doi.org/10.1002/qj.828>
- Finney, D.L., Marsham, J.H., Jackson, L.S., Kendon, E.J., Rowell, D.P., Boorman, P.M., Keane, R.J., Stratton, R.A. and Senior, C.A. (2019) Implications of improved representation of convection for the East Africa water budget using a convection-permitting model. *Journal of Climate*, 32(7), 2109–2129. <https://doi.org/10.1175/JCLI-D-18-0387.1>
- Funk, C., Peterson, P., Landsfeld, M., Pedreros, D., Verdin, J., Shukla, S., Husak, G., Rowland, J., Harrison, L., Hoell, A. and Michaelsen, J. (2015) The climate hazards infrared precipitation with stations – A new environmental record for monitoring extremes. *Scientific Data*, 2, 1–21. <https://doi.org/10.1038/sdata.2015.66>
- Giannini, A., B. Lyon, R. Seager and N. Vigaud (2018) Dynamical and thermodynamic elements of modeled climate change at the East African margin of convection. *Geophysical Research Letters*, 45, 992–1000. <https://doi.org/10.1002/2017GL075486>
- Gill, A.E. (1980) Some simple solutions for heat-induced tropical circulation. *Quarterly Journal of the Royal Meteorological Society*, 106, 447–462
- The Guardian (2018). Lethal flash floods hit East African countries already in dire need, London. Available at: <https://www.theguardian.com/global-development/2018/may/08/deadly-flash-floods-east-africa-dire-need-kenya-rwanda-somalia>, accessed 4 June 2019.
- Hoell, A., Hoerling, M., Eischeid, J., Quan, X.-W. and Liebmann, B. (2017) Reconciling theories for human and natural attribution of recent East Africa drying. *Journal of Climate*, 30(6), 1939–1957. <https://doi.org/10.1175/JCLI-D-16-0558.1>
- Hogan, E., Shelly, A. and Xavier, P. (2015) The observed and modelled influence of the Madden–Julian Oscillation on East African rainfall. *Meteorological Applications*, 22(3), 459–469. <https://doi.org/10.1002/met.1475>
- Huffman, G.J., Bolvin, D.T., Nelkin, E.J., Wolff, D.B., Adler, R.F., Gu, G., Hong, Y., Bowman, K.P. and Stocker, E.F. (2007) The TRMM multisatellite precipitation analysis (TMPA): quasi-global, multi-year, combined-sensor precipitation estimates at fine scales. *Journal of Hydrometeorology*, 8(1), 38–55. <https://doi.org/10.1175/JHM560.1>
- Jackson, L.S., Keane, R.J., Finney, D.L., Marsham, J.H., Parker, D.J., Senior, C.A. and Stratton, R.A. (2019) Regional differences in the response of rainfall to convectively coupled Kelvin waves over tropical Africa. *Journal of Climate*, 32, 8143–8165. <https://doi.org/10.1175/JCLI-D-19-0014.1>
- Kilavi, M., MacLeod, D., Ambani, M., Robbins, J., Dankers, R., Graham, R., Titley, H., Salih, A.A.M. and Todd, M.C. (2018) Extreme rainfall and flooding over Central Kenya including Nairobi City during the Long-Rains season 2018: causes, predictability, and potential for early warning and actions. *Atmosphere*, 9(12), 472–501. <https://doi.org/10.3390/atmos9120472>
- Klotzbach, P.J. (2014) The Madden–Julian Oscillation's impacts on worldwide tropical cyclone activity. *Journal of Climate*, 27(6), 2317–2330. <https://doi.org/10.1175/JCLI-D-13-00483.1>
- Knutson, T.R., McBride, J.L., Chan, J., Emanuel, K.A., Holland, G., Landsea, C., Held, I.M., Kossin, J.P., Srivastava, A.K. and Sugi, M.

- (2010) Tropical cyclones and climate change. *Nature Geoscience*, 3(3), 157–163. <https://doi.org/10.1038/ngeo779>
- Levinson, D.H., Knapp, K.R., Kruk, M.C., Diamond, H.J. and Kossin, J.P. (2010). The International Best Track Archive for Climate Stewardship (IBTrACS) project: overview of methods and Indian Ocean statistics, pp. 215–221 in *Indian Ocean Tropical Cyclones and Climate Change*. Charabi, Y. (ed.), Springer, Dordrecht, Netherlands.
- Liebmann, B. and Smith, C.A. (1996) Description of a complete (interpolated) outgoing longwave radiation dataset. *Bulletin of the American Meteorological Society*, 77(6), 1275–1277
- Maidment, R.I., Allan, R.P. and Black, E. (2015) Recent observed and simulated changes in precipitation over Africa. *Geophysical Research Letters*, 42(19), 8155–8164. <https://doi.org/10.1002/2015GL065765>
- Matsuno, T. (1966) Quasi-geostrophic motions in the Equatorial area. *Journal of the Meteorological Society of Japan, series II*, 44(1), 25–43. https://doi.org/10.2151/jmsj1965.44.1_25
- Mwangi, E., Mungai, J. and Chanzu, B. (2018). GCRF African SWIFT report on flooding and heavy rainfall in Kenya, May 2018. <https://africanswift.org/2018/05/>, accessed 14 November 2019.
- Nakamura, K. (1968) Equatorial westerlies over East Africa and their climatological significance. *Geographical Review of Japan*, 41(6), 359–373. <https://doi.org/10.4157/grj.41.359>
- Nicholson, S.E. (1996). A review of climate dynamics and climate variability in eastern Africa, in *The limnology, climatology and paleoclimatology of the East African lakes*, pp. 25–56. Johnson, T.C., Odada, E.O. (eds), Gordon and Breach, Amsterdam, Netherlands.
- Nicholson, S.E. (2017) Climate and climatic variability of rainfall over eastern Africa. *Reviews of Geophysics*, 55(3), 590–635. <https://doi.org/10.1002/2016RG000544>
- Pohl, B. and Camberlin, P. (2006) Influence of the Madden–Julian Oscillation on East African rainfall. I: Intraseasonal variability and regional dependency. *Quarterly Journal of the Royal Meteorological Society*, 132, 2521–2539. <https://doi.org/10.1256/qj.05.104>
- Rowell, D.P., Booth, B.B.B., Nicholson, S.E. and Good, P. (2015) Reconciling past and future rainfall trends over East Africa. *Journal of Climate*, 28(24), 9768–9788. <https://doi.org/10.1175/JCLI-D-15-0140.1>
- Shanko, D. and Camberlin, P. (1998) The effects of the southwest Indian Ocean tropical cyclones on Ethiopian drought. *International Journal of Climatology*, 18(12), 1373–1388. [https://doi.org/10.1002/\(SICI\)1097-0088\(1998100\)18:12<1373::AID-JOC313>3.0.CO;2-K](https://doi.org/10.1002/(SICI)1097-0088(1998100)18:12<1373::AID-JOC313>3.0.CO;2-K)
- Vellinga, M. and Milton, S.F. (2018) Drivers of interannual variability of the East African “Long Rains”. *Quarterly Journal of the Royal Meteorological Society*, 144, 861–876. <https://doi.org/10.1002/qj.3263>
- Vizy, E.K. and Cook, K.H. (2019) Observed relationship between the Turkana low-level jet and boreal summer convection. *Climate Dynamics*, 53, 4037–4058. <https://doi.org/10.1007/s00382-019-04769-2>
- Wainwright, C.M., Marsham, J.H., Keane, R.J., Rowell, D.P., Finney, D.L., Black, E. and Allan, R.P. (2019) ‘Eastern African Paradox’ rainfall decline due to shorter not less intense Long Rains. *npj Climate and Atmospheric Science*, 2(1), 1–9. <https://doi.org/10.1038/s41612-019-0091-7>
- Walker, D.P., Birch, C.E., Marsham, J.H., Scaife, A.A., Graham, R.J. and Segele, Z.T. (2019) Skill of dynamical and GHACOF consensus seasonal forecasts of East African rainfall. *Climate Dynamics*, 53, 4911–4935. <https://doi.org/10.1007/s00382-019-04835-9>
- Walsh, K.J.E., McBride, J.L., Klotzbach, P.J., Balachandran, S., Camargo, S.J., Holland, G., Knutson, T.R., Kossin, J.P., Lee, T.-C., Sobel, A. and Sugi, M. (2016) Tropical cyclones and climate change. *Wiley Interdisciplinary Reviews: Climate Change*, 7(1), 65–89. <https://doi.org/10.1002/wcc.371>
- Wheeler, M.C. and Hendon, H.H. (2004) An all-season real-time multivariate MJO index: development of an index for monitoring and prediction. *Monthly Weather Review*, 132(8), 1917–1932. [https://doi.org/10.1175/1520-0493\(2004\)132<1917:AARMMI>2.0.CO;2](https://doi.org/10.1175/1520-0493(2004)132<1917:AARMMI>2.0.CO;2)
- Woodhams, B.J., Birch, C.E., Marsham, J.H., Lane, T.P., Bain, C.L. and Webster, S. (2019) Identifying key controls on storm formation over the Lake Victoria basin. *Monthly Weather Review*, 147(9), 3365–3390. <https://doi.org/10.1175/mwr-d-19-0069.1>
- Yang, W., Seager, R., Cane, M.A. and Lyon, B. (2015) The annual cycle of East African precipitation. *Journal of Climate*, 28(6), 2385–2404. <https://doi.org/10.1175/JCLI-D-14-00484.1>

How to cite this article: Finney DL, Marsham JH, Walker DP, *et al.* The effect of westerlies on East African rainfall and the associated role of tropical cyclones and the Madden–Julian Oscillation. *Q.J.R. Meteorol. Soc.* 2020;146:647–664. <https://doi.org/10.1002/qj.3698>